


Edge-to-Stem Variability in Wet-Canopy Evaporation From an Urban Tree Row

John T. Van Stan II¹  · Zachary Norman¹ · Adrian Meghoo¹ · Jan Friesen² · Anke Hildebrandt³ · Jean-François Côté⁴ · S. Jeffrey Underwood⁶ · Gustavo Maldonado⁵

Received: 20 October 2016 / Accepted: 20 June 2017 / Published online: 7 July 2017
© Springer Science+Business Media B.V. 2017

Abstract Evaporation from wet-canopy (E_C) and stem (E_S) surfaces during rainfall represents a significant portion of municipal-to-global scale hydrologic cycles. For urban ecosystems, E_C and E_S dynamics play valuable roles in stormwater management. Despite this, canopy-interception loss studies typically ignore crown-scale variability in E_C and assume (with few indirect data) that E_S is generally <2% of total wet-canopy evaporation. We test these common assumptions for the first time with a spatially-distributed network of in-canopy meteorological monitoring and 45 surface temperature sensors in an urban *Pinus elliotii* tree row to estimate E_C and E_S under the assumption that crown surfaces behave as “wet bulbs”. From December 2015 through July 2016, 33 saturated crown periods (195 h of 5-min observations) were isolated from storms for determination of 5-min evaporation rates ranging from negligible to 0.67 mm h^{-1} . Mean E_S (0.10 mm h^{-1}) was significantly lower ($p < 0.01$) than mean E_C (0.16 mm h^{-1}). But, E_S values often equalled E_C and, when scaled to trunk area using terrestrial lidar, accounted for 8–13% (inter-quartile range) of total wet-crown evaporation ($E_S + E_C$ scaled to surface area). E_S contributions to total wet-crown evaporation maximized at 33%, showing a general underestimate (by 2–17 times) of this quantity in the literature. Moreover, results suggest wet-crown evaporation from urban tree rows can be adequately estimated by simply assuming saturated tree surfaces behave as wet bulbs, avoiding problematic assumptions associated with other physically-based methods.

✉ John T. Van Stan II
jvanstan@georgiasouthern.edu

¹ Department of Geology and Geography, Georgia Southern University, Statesboro, GA, USA

² Department of Catchment Hydrology, Helmholtz Centre for Environmental Research – UFZ, Leipzig, Germany

³ Institute of Geoscience, Friedrich Schiller University Jena, Jena, Germany

⁴ Canadian Wood Fibre Centre, Natural Resources Canada, Québec, QC, Canada

⁵ Department of Civil Engineering and Construction Management, Georgia Southern University, Statesboro, GA, USA

⁶ Office of the Vice President for Research, California State University, Los Angeles, CA, USA

Keywords *Pinus elliottii* · Rainfall interception · Tree surface temperature · Urban forest · Wet-canopy evaporation · Wet-bulb temperature

1 Introduction

Forests intercept and evaporate significant amounts of rainfall, depending on canopy structure (leaf area index, bark structure, etc.) and storm conditions (rainfall amount and intensity, wind conditions, etc.). Canopy rainfall interception, therefore, plays an important role in the stormwater management of urban ecosystems (Wang et al. 2008). In a statewide (California, USA) assessment, rainfall interception losses from urban trees reduced stormwater by $26 \times 10^6 \text{ m}^3 \text{ year}^{-1}$ —an ecosystem service valued annually at $>\$41$ million for reduced runoff, municipal stormwater treatment, and flood control costs (McPherson et al. 2016). As a result of the hydro-economic value of urban-canopy rainfall interception, current research efforts have begun unifying afforestation strategies (Kimbauer et al. 2013; Sadeghi et al. 2016) and common selection criteria (shade, pest/disease resistance, pollution resistance, etc.) for landscaping species (Van Stan et al. 2015; Holder and Gibbes 2017) with urban-water-resource management objectives. To our knowledge, this is limited by a lack of results on the most common urban forest structure, landscaped tree rows, in favour of a focus on individual trees or tree components (e.g., Xiao et al. 2000; Guevara-Escobar et al. 2007; Pereira et al. 2009; Livesley et al. 2014; Holder and Gibbes 2017). This is surprising, since landscaped tree rows are a prevalent structure in urban ecosystems—lining streets, swales, medians, parking lots, and providing privacy screens between residential properties.

Canopy-interception-loss processes commence when rain droplets contact tree surfaces, being stored there until draining to the stem, to the floor via throughfall, or until evaporated. Intercepted rainwater that drains to the stem generates stemflow once the storage capacity of stem bark and epiphytes, if present, reaches saturation. Thus, traditional conceptual ideas of canopy-interception-loss processes have separated wet-crown evaporation sources into water stored on canopy and stem surfaces (Valente et al. 1997; van Dijk and Bruijnzeel 2001; Carlyle-Moses and Gash 2011). Together, total wet-crown evaporation (stem evaporation (E_S) + canopy evaporation (E_C) scaled to surface area) is a significant proportion (10%) of global average precipitation (Dirmeyer et al. 2006) and its estimation contributes large uncertainty to global water-balance estimates (Miralles et al. 2010). These evaporative fluxes can also regionally conserve rainfall (van der Ent et al. 2014) since they recycle moisture at shorter time scales than other atmospheric water sources, i.e., transpiration (Wang-Erlandsson et al. 2014). As such, an improved understanding of the variability of wet-crown evaporation beyond the current binary E_C versus E_S conceptualization is merited.

During the early conceptualization, application and evaluation stages of canopy-interception-loss models, either net precipitation observations were assessed to conclude that E_S was very small, only 2% of E_C (Rutter and Morton 1977), or E_S was simply considered negligible (Gash 1979). However, leafless interception losses exceeding stem storage (e.g., Dolman 1987) indicated that E_S plays a more substantive role, and gained some attention during the reformulation of canopy-interception-loss models (Valente et al. 1997; van Dijk and Bruijnzeel 2001). Parametrizing E_S improved the performance of analytical models, yet since this improvement two fundamental questions remain unanswered: (1) can we more directly assess the difference between E_C and E_S ? and (2) how significant is canopy edge-to-stem variability in wet-crown evaporation? Answering these questions should fill a fundamental knowledge gap in the canopy hydrometeorological community that has persisted due to the ease of indirect estimates via net precipitation-versus-precipitation regression tech-

niques (Friesen et al. 2015). The reliance on estimates of interception-loss variables using solely net precipitation data can be problematic since they may contain significant error. For example, canopy water storage is many times higher when estimated with more “direct” observations (stem compression) than standard net precipitation-based regression techniques (Friesen et al. 2008, 2015). New methods now exist relying on more direct observations to estimate evaporation from saturated tree surfaces, including one based on a simple assumption (wet tree surfaces behave as wet bulbs) verifiable with inexpensive temperature sensors (Pereira et al. 2009, 2016).

Assuming a landscaping tree row on an otherwise open urban landscape is well-ventilated (Pereira et al. 2016), we can test hypotheses tenuously supported by indirect net precipitation data (but generally accepted in the forest hydrometeorological community) by measuring surface temperatures throughout the canopy after saturation. Our study, therefore, uses a spatially-distributed network of in-canopy meteorological and surface temperature sensors to test whether (hypothesis 1) E_S is significantly smaller than E_C , and (hypothesis 2) canopy edge-to-stem variability in evaporation rates from saturated tree crowns is substantial and predictable. In testing these hypotheses, we report the first estimates of a major component of the urban hydrological cycle (E_C and E_S) for a dominant forest structure in urban ecosystems (landscaping tree rows).

2 Materials and Methods

2.1 Study Site and Meteorological Monitoring

The instrumented landscaping tree row (Fig. 1a) is exclusively composed of *Pinus elliottii* (Englem., slash pine) and located on the Georgia Southern University campus along the southbound lane of Akins Boulevard in Statesboro, Georgia, USA (32.4158 N, 81.7906 W). The climate is humid sub-tropical with no distinct dry season (Köppen *Cfa*) and a mean annual (1925–2014) rainfall of 1170 mm (University of Georgia Weather Network 2016). Rainfall is the dominant form of precipitation and accounts for all precipitation observed during the study period. As mean minimum monthly temperatures are above 0 °C throughout the year (lowest is 3.5 °C in January), snowfall is negligible (University of Georgia Weather Network 2016). Mean monthly total rain amounts are relatively uniform for 8 months of the year (60–100 mm month⁻¹), but increase to 110–150 mm month⁻¹ from June to September due to frequent thunderstorms. Canopy radii were approximately 3 m; through terrestrial lidar scans (more details on terrestrial lidar methods provided in Sect. 2.3), average tree height was 13.9 m and average diameter at breast height (*dbh*) was 0.42 m (± 0.04 m standard deviation). Lidar-derived diameter at breast height (*dbh*) measurements were manually checked and values compared well (± 0.01 m difference).

The study period lasted 8 months, beginning December 2015 and ending July 2016. A continuously recording meteorological station was situated on-site (370 m west of the tree row), in a clearing surrounded by grass sport fields, and equipped with three tipping bucket gauges (TE-525MM, Texas Electronics, Dallas, Texas, USA), a pyranometer (CMP6, Kipp & Zonen, Delft, The Netherlands), a two-axis ultrasonic wind speed and direction sensor (Wind-Sonic, Gill, Hampshire, UK), and an air temperature/relative humidity probe (HMP155, Vaisala, Vantaa, Finland). All meteorological station sensors were interfaced with a data-logger (CR1000, Campbell Scientific, Logan, Utah, USA) to record observations at 5-min intervals. Elevation of the meteorological station was 6.1 m above the ground to be at an elevation as close to the centre of the tree-row canopy as possible (and to prevent vandal-

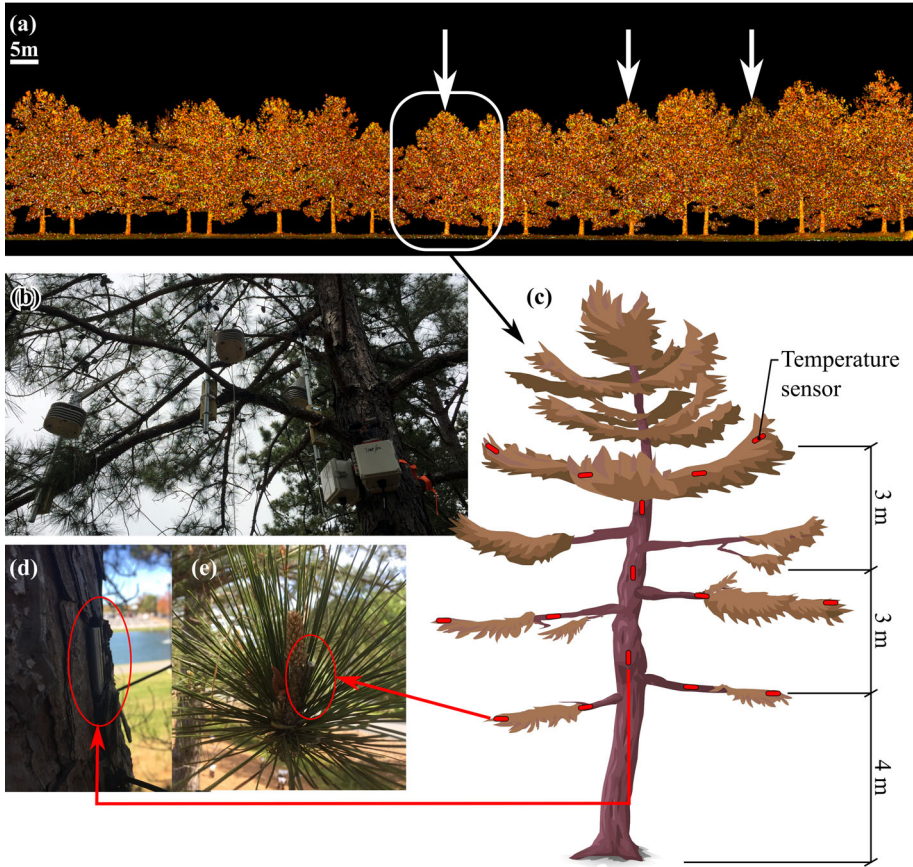


Fig. 1 Akins Boulevard landscaping tree row **a** terrestrial lidar point cloud showing the three trees selected for installation of **b** in-canopy meteorological monitoring and **c** distributed surface temperature measurements with example photographs of sensors installed **d** on the stem and **e** within leaves

ism). Meteorological monitoring was installed within the canopy at the same elevation and at 2, 1 m, and zero distance from the stem (Fig. 1b) to log (model H21-002) edge-to-stem variability every 5 min in air temperature and relative humidity (model S-THB-M002), radiation (model S-LIB-M003) and wind speed (model S-WSB-M003)—all equipment by HOBO (Onset Computer, Bourne, Massachusetts, USA). Temperature and relative humidity sensors for meteorological observations were placed in radiation shields (HOBO model RS3-B).

2.2 Wet-Canopy and Wet-Stem Evaporation Rates

Pereira et al. (2009) found that the temperature of well-ventilated tree surfaces that are fully saturated by rainfall approaches the wet-bulb temperature, allowing the wet-surface evaporation rate (E , $\text{kg m}^{-2} \text{s}^{-1}$) to be estimated as,

$$\lambda E = \frac{\rho_a c_p}{\gamma} g_b v (e_s(T_s) - e_a) \tag{1}$$

where λ is the latent heat of vapourization (J kg^{-1}), ρ_a is the air density (kg m^{-3}), c_p is the air specific heat at constant pressure ($\text{J kg}^{-1} \text{K}^{-1}$), γ is the psychrometric constant (Pa K^{-1}), $e_s(T_s)$ is the saturation vapour pressure (Pa) at the surface temperature (T_s , K), e_a is the actual vapour pressure of surrounding air, and g_{bV} is the aerodynamic conductance (m s^{-1}) for the mean boundary-layer conductance for water vapour of leaves (g_{lV}) and stems (g_{sV}) (Monteith and Unsworth 2008; Pereira et al. 2009) with wind-speed data at each location, from the edge to the interior, using the open weather station (for the edge) and in-canopy meteorological monitoring for mid-canopy and stem locations (Fig. 1b). With Eq. 1, measured T_s can be used directly, T_s can be computed from available energy and air wet-bulb temperature (see Eq. 2 of Pereira et al. 2016), or assumed equal to nearby wet-bulb temperatures, as supported in results from recent coupled water-energy balance work (van Dijk et al. 2015).

Two relations were developed to relate g_{lV} and g_{sV} to wind speed (u), assuming both canopy elements are well-represented by cylinder geometry with characteristic dimensions of 0.0015 m diameter for needles and the mean dbh (0.416 m) for stems. This yielded,

$$g_{lV} = 0.072u^{0.47} \frac{k}{D}, \quad (2)$$

$$g_{sV} = 0.0054u^{0.60} \frac{k}{D}, \quad (3)$$

where k is the thermal conductivity of air and D is the water vapour diffusivity in air, giving a ratio of 1.08 for the laminar boundary layer. Since needleleaves shelter each other, the prediction is overestimated and requires a reduction factor; we used 0.4 as the g_{lV} reduction factor (Monteith and Unsworth 2008; Pereira et al. 2016). We are unaware of any reduction or enhancement factor necessary for g_{sV} , so g_{lV} and g_{sV} were then scaled to ceptometer-derived leaf area index (LAI) corrected to canopy cover fraction ($c = 75.3\%$) and terrestrial lidar-derived woody area index (WAI) of the stems corrected to stem-cover fraction ($s = 1.9\%$), respectively, to generate the bulk aerodynamic conductance of leaves (g_{blV}) and stems (g_{bsV}),

$$g_{blV} = g_{lV} \text{LAI}/c, \quad (4)$$

$$g_{bsV} = g_{sV} \text{WAI}/s \quad (5)$$

We directly measured T_s for 45 total locations, with 15 temperature sensors installed in each of three randomly selected tree crowns in the landscaped tree row (Fig. 1c). Temperature sensors were installed at three different heights (4, 7, and 10 m above ground; Fig. 1c) with 10 m being the maximum height accessible by the available vehicular-elevated work platform. At each height for each tree, two branches were selected for installation of one sensor each at the branch edge, branch middle, and on the stem at distances from the stem corresponding to the in-canopy meteorological monitoring (Fig. 1c). T_s observations were made using inexpensive, pre-wired and waterproofed DS18B20 digital temperature sensors (Adafruit, product 381, New York, New York, USA) (Fig. 1d, e). Sensors were interfaced with a custom datalogger consisting of an Arduino mega 2560, secure digital (SD) card shield, and liquid crystal display (LCD) shield (Arduino, Somerville, Massachusetts, USA) and were powered external to the Arduino by a 12 volt to 5 volt buck converter. The Arduino-based datalogger polled T_s sensors every 5 min as determined by the built-in-clock (sync'd to the same time as the meteorological station and in-canopy meteorological equipment), then recorded data to an SD card. Data from the open weather station were used to estimate E_c for T_s sensors installed on needles at the canopy edge, whereas the nearest in-canopy meteorological data were used to estimate E_c for mid-canopy T_s sensors. In-canopy meteorological data near the stem were used to estimate E_s for sensors installed on stems. T_s sensor failures occurred for

one stem sensor at the 7-m elevation, and three edge sensors at the 4-m elevation, one on each tree.

Thirty-three periods, representing just over 195 h of 5-min observations, where the tree crowns are considered saturated by rainfall were isolated for analysis. Periods of crown saturation were defined as any time where both, (1) rainfall exceeded 0.002 m, the storage capacity as determined from standard net rainfall-versus-rainfall regression techniques (Friesen et al. 2015), and (2) the average of all T_s observations were within 5% of the wet-bulb temperature, computed as in Stull (2011).

2.3 Determination of Stem and Leaf Area

Vegetation surface area index (*SAI*) of the canopy was determined using an LAI-2200TC plant canopy analyzer (LiCOR, Lincoln, Nebraska, USA) consisting of two LAI-2250 wands (one levelled in the open and logging every minute for correction of manual measurements made by the second wand). LAI-2250 data points were collected every 10 m along three transects spaced approximately 2 m apart to cover the full width of canopy cover along the tree row. Each reading was taken while holding the sensor level at breast height (1.4 m) with a 90° lens mask. Leaf area index was derived from the two LAI-2250 observation records using the FV2200 software (LiCOR, Lincoln, Nebraska, USA). Since *LAI* derived in this way represents only half the surface area (Fassnacht et al. 1994; Smolander and Stenberg 1996), it was multiplied by 2 and then the leaf portion was corrected using a species-specific branch-to-leaf area ratio of 0.091 and clumping correction factor of 1.8 (Baynes and Dunn 1997). This resulted in a canopy $SAI = 7.71$, which compares well for *P. elliotii* site *SAI* values from Baynes and Dunn (1997) ranging from 4.1 to 9. Projected canopy area of the site was determined manually by measuring radii from eight directions (north, north-west, west, south-west, south, south-east, east, north-east) starting at the trunk and ending at the canopy edge, resulting in 124 m² total projected canopy area.

Terrestrial lidar scans were used to estimate stem surface area. They are able to collect large amounts of three-dimensional (3D) data on the fine-scale structure of trees and forest stands (Dassot et al. 2011). Advanced modelling techniques are used to extract information on the branching structure (e.g. Raunonen et al. 2013; Hackenberg et al. 2015). These techniques can be applied to provide reliable estimates of plant surface areas of individual trees assuming that the acquisition of lidar data was performed in optimal conditions: i.e., to minimize the occlusion where clustered or opaque objects prevent detection of elements in occluded areas, and noise or movement generated by wind.

A ScanStation C10 (Leica Geosystems, St. Gallen, Switzerland) was employed to capture lidar data and produce a georeferenced, 3D point cloud model of the urban tree row. With a maximum range of 300 m at 50,000 points s⁻¹, the C10 accuracy (1- to-50-m range) is 6 mm for position and 4 mm for distance. A 20 m × 90 m swath containing 17 trees was scanned from 12 scanning locations, six on each side of the tree row (Fig. 2). Each scan was set to medium resolution (3'26" angular resolution, or 0.1-m point spacing, horizontally and vertically, at 100 m). Several high-definition surveying twin-target pole systems and 0.1524-m, black-and-white, tilt- and -turn targets were placed and captured from each scan station to register individual scans into a common reference system. Target redundancy assisted in attaining a relatively low overall co-registration error of 0.005 m. For geo-referencing purposes, four benchmarks were established near the tree row (Fig. 2). Benchmark coordinates were acquired in the Georgia East State plane coordinate system via a Global Positioning System (Trimble Survey Controller-2 paired with a Global Navigation Satellite System-R6 receiver, Trimble Inc., Sunnyvale, California, USA). Canopy points were manually removed from all trees in

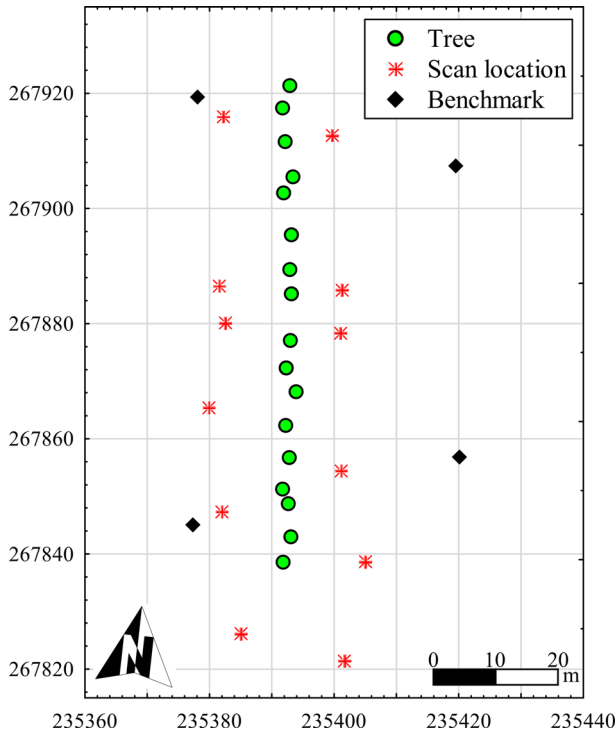


Fig. 2 Map of tree-row location with surrounding terrestrial lidar scanning positions and benchmarks. Coordinate system is North American datum 1983, high accuracy reference network, Georgia East State plane coordinate system

the co-registered lidar scan. Trimmed point clouds were imported into CompuTree 3.6.1.2b (<http://computree.onf.fr/>) and analyzed with the SimpleTree plugin (<http://www.simpletree.uni-freiburg.de/software.html>), which computed stem surface area by fitting cylinders to stem point clouds (Hackenberg et al. 2015). Stem surface area ranged from 10–17 m² per tree, and the ratio of total stem area to canopy area was 19.7%.

2.4 Statistical Analysis

Descriptive statistics were compiled for all hydrometeorological variables. Evaporation rates from the canopy edge, middle and stem were tested for significance between means by analysis of variance and Tukey-Kramer honest significant difference test after ensuring the data met underlying assumptions. Regressions testing correlation magnitude and significance between T_S observations and wet-bulb temperatures were performed.

3 Results

Meteorological conditions during the crown saturation periods widely varied. Minimum rainfall amount was 2.3 mm (just above the canopy water storage threshold), but the maximum magnitude of rainfall surpassed 100 mm (Table 1). Median rainfall intensity was 1.7 mm h⁻¹ (Table 1), which is considered “light” per the American Meteorological Society (AMS)

Table 1 Meteorological characteristics for periods of crown saturation and the hourly evaporation rates (E) derived from surface-temperature measurements for the canopy edge, middle, and stem locations

Event number	Event start Date/time (EST)	Rainfall (mm)	Intensity (mm h^{-1})	Radiation (W m^{-2})	Wind speed (m s^{-1})		E (mm h^{-1})		
					Mean	Max gust	Edge	Middle	Stem
1	22 Dec 2015 0900	3.0	1.5	10.1	1.1	4.3	0.08	0.08	0.06
2	22 Dec 2015 1900	6.4	0.4	4.6	0.6	2.8	0.04	0.04	0.04
3	23 Dec 2015 1700	11.0	0.5	8.1	1.2	10.0	0.24	0.24	0.19
4	29 Dec 2015 0800	4.5	1.4	17.8	1.6	4.1	0.08	0.06	0.04
5	31 Dec 2015 1800	6.3	1.6	13.0	1.4	5.7	0.33	0.32	0.24
6	1 Jan 2016 0100	21.2	1.9	0.0	1.0	4.1	0.09	0.09	0.05
7	1 Jan 2016 2000	21.7	0.9	7.3	1.4	5.3	0.14	0.14	0.08
8	8 Jan 2016 0400	6.7	1.1	2.6	2.4	6.5	0.17	0.18	0.13
9	15 Jan 2016 0700	23.4	5.8	6.6	2.1	14.5	0.24	0.28	0.26
10	4 Feb 2016 1800	105.8	5.3	6.6	1.4	8.9	0.12	0.08	0.04
11	6 Feb 2016 1300	4.7	1.2	110.2	2.3	9.9	0.21	0.19	0.10
12	7 Feb 2016 2000	11.0	0.9	0.0	3.4	11.8	0.37	0.34	0.25
13	16 Feb 2016 0300	9.6	2.4	0.2	1.7	5.7	0.17	0.17	0.11
14	24 Feb 2016 0500	28.0	7.0	0.1	3.4	9.8	0.28	0.31	0.20
15	3 Mar 2016 2200	10.9	1.4	0.0	2.7	12.9	0.38	0.34	0.10
16	13 Mar 2016 0600	2.3	0.3	30.1	1.5	7.2	0.13	0.13	0.04

Table 1 continued

Event number	Event start Date/time (EST)	Rainfall (mm)	Intensity (mm h ⁻¹)	Radiation (W m ⁻²)	Wind speed (m s ⁻¹)		<i>E</i> (mm h ⁻¹)		
					Mean	Max gust	Edge	Middle	Stem
17	18 Mar 2016 0000	7.7	1.5	0.1	1.4	8.8	0.20	0.23	0.12
18	26 Mar 2016 1400	2.8	0.5	74.9	1.9	9.2	0.18	0.05	0.04
19	12 Apr 2016 0400	2.5	0.6	1.6	0.9	2.4	0.09	0.08	0.01
20	12 Apr 2016 1400	4.9	0.7	128.6	1.0	3.4	0.07	0.06	0.01
21	2 May 2016 1500	45.1	9.8	34.1	1.0	5.8	0.33	0.30	0.28
22	3 May 2016 2000	55.1	3.4	0.4	1.1	2.0	0.44	0.44	0.33
23	29 May 2016 0000	48.6	3.8	16.1	1.9	3.4	0.11	0.09	0.07
24	29 May 2016 1600	49.8	3.1	79.3	1.0	3.7	0.05	0.05	0.03
25	4 Jun 2016 2300	15.7	8.2	0.2	0.7	0.8	0.16	0.14	0.07
26	6 Jun 2016 0800	51.2	3.1	44.2	0.4	0.5	0.04	0.03	0.04
27	28 Jun 2016 2100	39.6	18.3	0.3	1.4	1.5	0.02	0.02	0.05
28	30 Jun 2016 1700	4.5	3.6	35.0	0.8	1.5	0.13	0.11	0.08
29	6 Jul 2016 1800	3.0	1.7	23.0	1.7	5.7	0.06	0.04	0.02
30	9 Jul 2016 1600	4.2	5.6	21.3	1.1	4.7	0.05	0.04	0.02
31	15 Jul 2016 1800	7.0	7.6	49.5	1.6	2.7	0.16	0.15	0.14
32	16 Jul 2016 2000	48.7	11.2	0.3	1.4	5.3	0.08	0.07	0.05
33	19 Jul 2016 2100	6.5	4.6	0.3	0.1	0.5	0.05	0.03	0.02
	Mean:	20.4	3.6	22.0	1.5	5.5	0.16 ^a	0.15 ^a	0.10 ^b

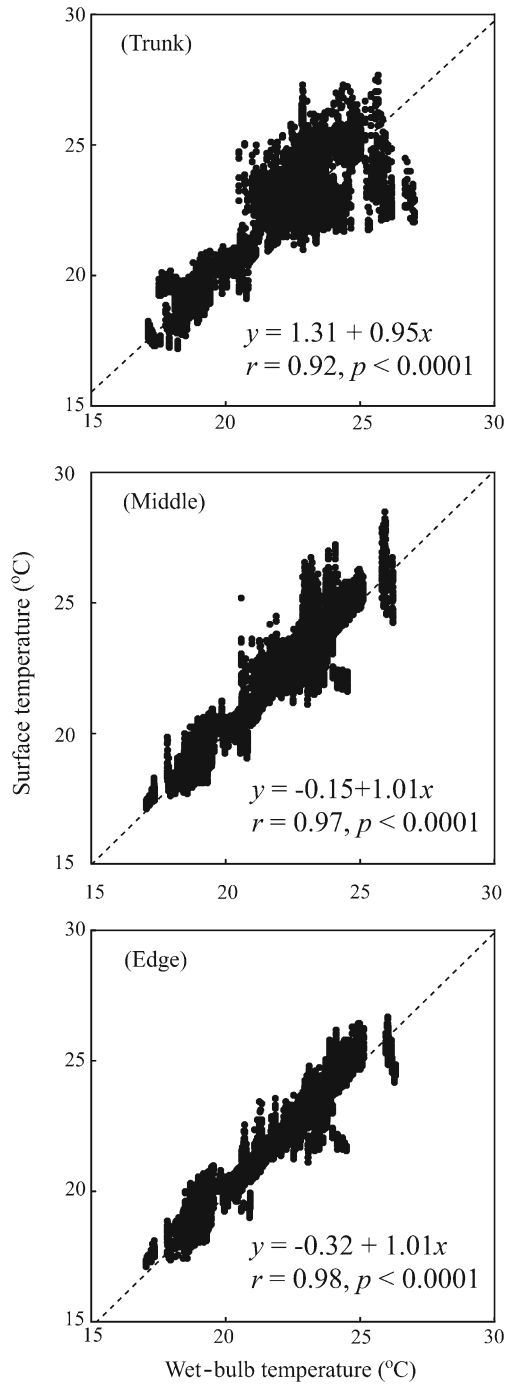
Mean values across hourly data are provided and superscripts indicate only stem *E* values significantly differed from middle and edge ($F = 6.29, p < 0.01$)

standards ($<2.51 \text{ mm h}^{-1}$). Many events during the study period fell into AMS moderate (27% between >2.5 and $\leq 7.5 \text{ mm h}^{-1}$) and heavy (15% $> 7.5 \text{ mm h}^{-1}$) intensity classes (Table 1). The mean hourly net radiation rarely exceeded 30 W m^{-2} and variability was low, with a standard error of 5.7 W m^{-2} (Table 1). Mean wind speed also varied little among storms and was 1.5 m s^{-1} for all events (Table 1). Despite relatively consistent mean wind speeds, maximum sustained wind gusts varied between very calm (0.5 m s^{-1}) to strong winds (14.5 m s^{-1}). 5-min wet bulb temperatures plotted against T_s measurements during periods of crown saturation were strongly and significantly correlated (Fig. 3). Stem T_s observations had the greatest disagreement between wet bulb temperatures under warmer crown saturation periods (as shown by large deviations from the 1:1 line), yet there was still a significant and strong correlation (Fig. 3).

Five-min evaporation rates from saturated tree crown surfaces ranged from 0 to 0.67 mm h^{-1} during the study period, with locations throughout the crown achieving mean hourly values on the upper end of this range (Table 1). Average E_S for all measured events was significantly lower than E_C for both the edge and interior, being about half the magnitude (Table 1). Edge and interior E_C were not statistically distinct; however, E_C derived from edge T_s observations were more often larger than interior estimates for individual events (Table 1). The maximum evaporation rate was observed for E_C at the canopy edge on 3 May 2016 and the negligible (basically null) estimates were only achieved by E_S (Table 1). Yet, E_S was frequently substantial (exceeding 0.20 mm h^{-1}) during rainfall amounts that saturated the crown (31 December 2015, 15 January 2016, 24 February 2016, 2 May 2016, 3 May 2016), but nearly 60% of the time E_S was small, below 0.05 mm h^{-1} (Table 1). When scaled to canopy and stem area, E_S contribution to total evaporation during the saturation period was on average, 11% with an interquartile range between 8 and 13% (Fig. 4). Maximum proportion of E_S contributions to total wet-crown evaporation was 33% (Fig. 4) during a period of very low evaporation, when rates were between 0.01 and 0.03 mm h^{-1} (Table 1).

Although E_S was significantly lower than E_C , an example storm shows that E_S can be as high as E_C near the edge or in the interior of the crown for the studied *P. elliotii* landscaped forest row (Fig. 5). Elevated E_S tends to occur during large storms with high rainfall intensity (Table 1). Please note that mean air temperature from all meteorological monitoring (outside and inside canopy) is used in Fig. 5 as air temperature observations were statistically indistinct ($p > 0.1$) regardless of being outside the canopy, on the canopy edge, in the canopy middle, or near the trunk (i.e., interquartile range of standard error between measurements was $0.05\text{--}0.3^\circ\text{C}$). Crown surface temperatures early in the 2 May 2016 storm were larger than mean air temperature, but quickly fell below mean air temperature with the first rainfall pulse that saturated the crowns (Fig. 5a). Once leaf and stem surface temperatures dropped, they followed the average wet-bulb temperature of the surrounding air well (Fig. 5a). The greatest depression in T_s was at the canopy-edge location (Fig. 5a), agreeing with general trends reported in Table 1. Net radiation was also diminished as the cloud cover associated with each rainfall pulse appeared (Fig. 5b). As rain pulses ended, increased radiation due to reduced cloud cover led to warmed crown surfaces, but T_s remained below mean air temperature while saturation persisted after rain pulses (Fig. 5a, b). Note that although actual evaporation may be influenced by R_n , E_s and E_c estimates depended on wet-bulb temperatures and wind speed. Large sustained wind gusts are observed before and after rainfall pulses (Fig. 5c), which enables surfaces to dry in concert with radiation exposure and produces two pronounced peaks in wet-canopy evaporation (Fig. 3d). Most occurrences of E_S in the normal range of E_C ($0.1\text{--}0.4 \text{ mm h}^{-1}$) are observed under these conditions, with some exceptions where either wind gusts were low but rain intensity was high (e.g., 5 June 2016) or rain intensity was low but wind gusts were very high (e.g., 7 February 2016) (Table 1). It is worth noting

Fig. 3 Scatterplots showing strong relationships between wet-bulb temperatures and tree surface temperatures at the (*top*) stem, (*centre*) canopy middle, and (*bottom*) canopy edge isolated from periods considered saturated by rainfall



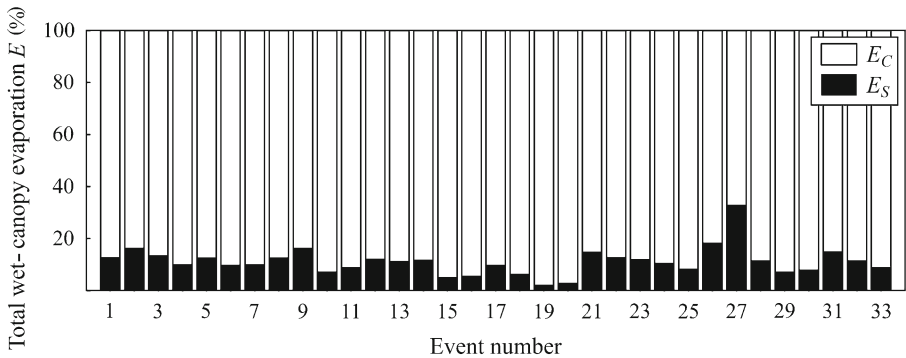


Fig. 4 Area-scaled proportion of total wet-crown evaporation loss for the canopy (E_C) and stem (E_S) for all monitored storms

the minor (5–10 min) offset between R_n measured outside the canopy versus the mid-canopy and trunk measurements (Fig. 5b). Possibilities were examined (consistent levelling of the sensor, time lag due to branch sway, or time differences between the Campbell, Arduino, and Hobo loggers), but none explained the minor offset in timing of canopy edge R_n . We expect this offset may be from the timing of clouds and branch/leaf material blocking sunlight.

4 Discussion

Results show that all portions of the tree (including the stem) were able to contribute measurably to wet-crown evaporation in a well-ventilated landscaped tree row (Table 1; Fig. 4). Estimates of E_S and both the interior and edge E_C from our landscaping tree row matched E_{PM} estimates well on average (Table 1), as was also reported by Pereira et al. (2016) for forest canopies favourably structured for permitting air circulation. This indicates that for a very common urban and suburban forest structure the minimally data-demanding wet-bulb approach may be applied. As the species at our site (*P. elliotii*) has a more “closed” canopy structure than most broadleaved species (see point cloud representation in Fig. 1a), the strong correlation between our wet-crown surface and wet-bulb temperatures (Fig. 3) suggest the applicability of the wet-bulb approach may also extend to common broadleaved species planted in landscaping tree rows. Estimating E_C and E_S in urban forest rows per the wet-bulb method also avoids violating (or attempting to satisfy) one-dimensional transfer model assumptions (Pereira et al. 2009).

Within the tree-row canopy, E_S was found to frequently approach, or equal, E_C values (rejecting hypothesis 1: Table 1; Fig. 4) under favourable storm conditions (e.g., Fig. 5). High rainfall intensity and elevated wind-gust speeds were generally necessary to not only saturate stem surfaces deep into the canopy (a process linked to increased stem-flow production across forest types: Crockford and Richardson 2000; Levia et al. 2011), but also evaporate stored rainwater (Table 1; Figs. 4, 5) that could diminish stem-flow (Van Stan et al. 2014). The value of E_S/E_C is far larger (>10% on average) than has been historically reported, albeit these forests are considered closed canopy: e.g., negligible (Gash 1979) to 2% (Rutter and Morton 1977; Valente et al. 1997). More recent estimates of E_S/E_C , termed the stem evaporative coefficient (ϵ) in current analytical modelling work (Valente et al. 1997; Miralles et al. 2010), have continued to use the 2–3% estimate. When E_S is scaled to surface area to assess the stem’s proportion of total wet-crown evaporation, which has not been done to date (e.g.,

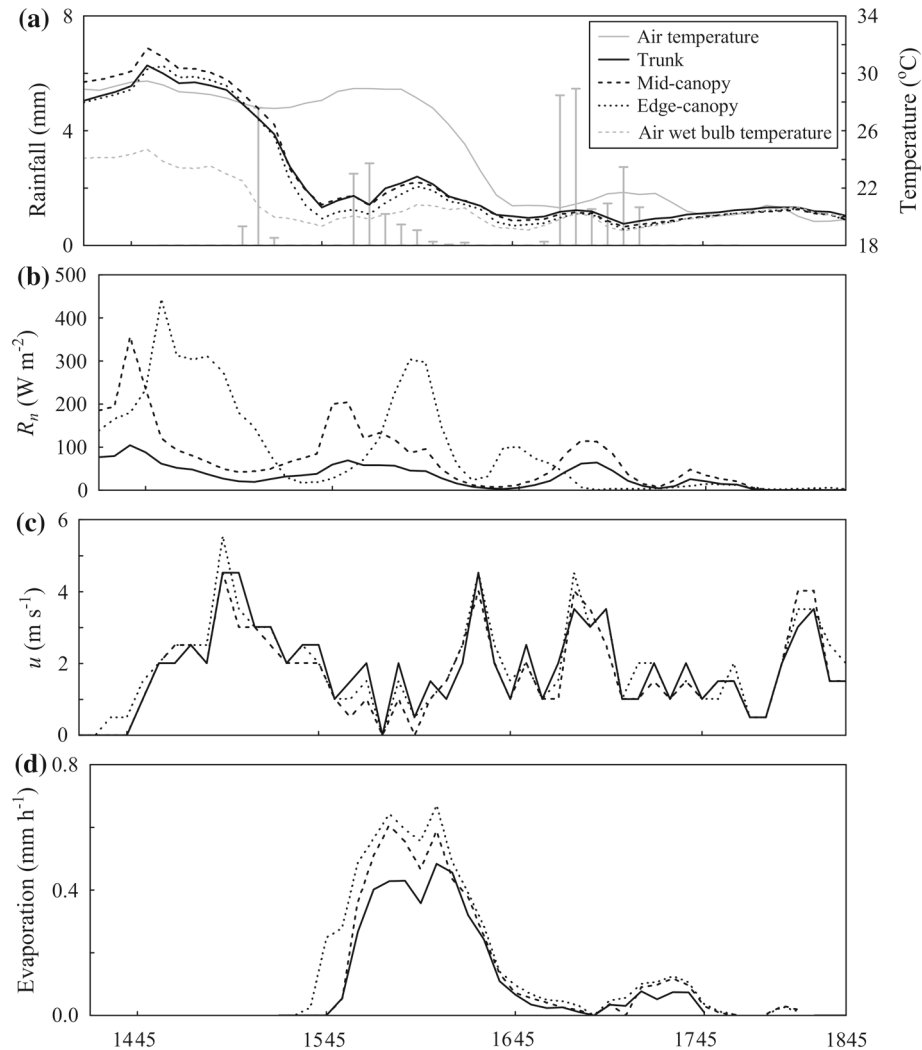


Fig. 5 5-min meteorological, tree surface temperature and hydrological data from an example saturation period on 2 May 2016 where E_S achieved evaporation rates comparable to those observed at the canopy edge and interior

van Dijk and Bruijnzeel 2001), E_S often exceeds >10% of total wet-crown evaporation for our site representing a common urban forest structure. These E_S proportions exceed estimates from previous studies by a factor of five (Linhoss and Siegert 2016), and over an order of magnitude during intense rainfall under windy conditions (Table 1; Fig. 4). This significantly underestimated E_S range (due to uncertainty) likely influences model sensitivity analyses (i.e., Linhoss and Siegert 2016) that could shift focus away from improvement in understanding of an important, yet neglected, forest canopy hydrometeorological variable.

We had expected wet-crown evaporation to increase from the stem to the exterior (hypothesis 2), but no significant difference was observed in E_C between the edge and interior of the canopy (Table 1). As saturated crown periods occur after establishment of rainfall (and

associated cloud cover), E_C is often affected by aerodynamic processes (Dunin et al. 1988; Holwerda et al. 2012). Thus, the expectation was that horizontal canopy wind-speed profiles would mirror those observed in the vertical dimension, diminishing with distance and resulting in decreasing E_C from edge to interior. Vertical wind-speed profiles abound (Oliver 1971; Syka and Starzak 2013), yet there are few horizontal wind-speed profiles within forest canopies (Xu et al. 2015) and the authors are aware of no measured horizontal wind profiles for urban trees or landscaping rows. In cases of strong winds (Fig. 5), wind speeds are minimally reduced. But, generally it appears that meteorological conditions driving evaporative losses in well-ventilated canopies decrease rapidly between the mid-canopy and trunk as radiation is intercepted and wind speed decreases due to near-stem biomass. This agrees with previous work on bark water storage (and, primarily, its relation to stem flow generation) suggesting that water stored on stem surfaces is often “sheltered” from meteorological effects during common storm conditions (Herwitz 1985; Levia and Herwitz 2005; Van Stan et al. 2016). Clearly, there is significant value in lidar beyond the trunk-surface-area measurements performed herein, including the measurement of fine-scale canopy structure elements that influence meteorological factors and their effect on wet-crown evaporation (like branch inclination angle and diameter, leaf and branch vertical and horizontal distribution, bark microrelief, etc.).

5 Conclusions

Our spatially-distributed network of in-canopy meteorological and surface temperature sensors found that evaporation from stems saturated by rainfall (E_S) was five times (on average) and 17 times (at its maximum) greater than previous indirect estimates. E_S values may equal those at the saturated canopy edge or interior (E_C). Under high wind-speed and rain-intensity conditions, E_S may even reach rates above 0.2 mm h^{-1} . These results show that crown-scale variability in evaporation between the canopy and stem is significant, but existing assumptions regarding the magnitude of E_S (generally being $<2\%$ of total crown evaporation) may be invalid for most storm conditions. To our knowledge, this study reports the first E_C and E_S estimates (a major component of the urban hydrological cycle) using the more “direct” crown-surface-temperature measurement technique for landscaping tree rows (a major urban forest structure). Results also suggest that, for a common urban and suburban forest structure, wet-crown evaporation can be adequately estimated using wet-bulb temperatures.

Acknowledgements This work was supported by the US-NSF (EAR-1518726). Student support for Zachary Norman was provided by the Environmental Protection Division of the Georgia Department of Natural Resources (EPD-WQ-5419). The authors thank the Georgia Southern University physical plant for assistance installing, maintaining and securing sensors within the canopy, and students Daniel Cirincione, Ravon Elam, Dylan Mesta, and Sandra Yankine for assistance with terrestrial lidar data collection and processing.

References

- Baynes J, Dunn GM (1997) Estimating foliage surface area index in 8-year-old stands of *Pinus elliotii* var. *elliottii* x *Pinus caribaea* var. *hondurensis* of variable quality. *Can J For Res* 27:1367–1375
- Carlyle-Moses D, Gash JHC (2011) Rainfall interception loss by forest canopies. Chapter 20 in: *Forest hydrology and biogeochemistry: synthesis of past research and future directions*. Springer, Heidelberg, pp 407–423
- Crockford RH, Richardson DP (2000) Partitioning of rainfall into throughfall, stemflow and interception: effect of forest type, ground cover and climate. *Hydrol Process* 14:2903–2920

- Dassot M, Constant T, Fournier M (2011) The use of terrestrial LiDAR technology in forest science: application fields, benefits and challenges. *Ann For Sci* 68:959–974
- Dirmeyer PA, Gao X, Zhao M, Guo Z, Oki T, Hanasaki N (2006) GSWP-2: Multimodel analysis and implications for our perception of the land surface. *Bull Am Meteorol Soc* 87:1381–1397
- Dolman AJ (1987) Summer and winter rainfall interception in an oak forest. Predictions with an analytical and a numerical simulation model. *J Hydrol* 90:1–9
- Dunin F, O'Loughlin E, Reyenga W (1988) Interception loss from eucalypt forest: Lysimeter determination of hourly rates for long term evaluation. *Hydrol Process* 2:315–329
- Fassnacht KS, Gower ST, Norman JM, McMurtrie RE (1994) A comparison of optical and direct methods for estimating foliage surface area index in forests. *Agr For Meteorol* 71:183–207
- Friesen J, van Beek C, Selker J, Savenije HHG, van de Giesen N (2008) Tree rainfall interception measured by stem compression. *Water Resour Res* 44:W00D15
- Friesen J, Lundquist J, Van Stan JT (2015) Evolution of forest precipitation water storage measurement methods. *Hydrol Process* 29:2504–2520
- Gash JHC (1979) An analytical model of rainfall interception by forests. *Q J R Meteorol Soc* 105:43–55
- Guevara-Escobar A, Gonzalez-Sosa E, Veliz-Chavez C, Ventura-Ramos E, Ramos-Salinas M (2007) Rainfall interception and distribution patterns of gross precipitation around an isolated *Ficus benjamina* tree in an urban area. *J Hydrol* 333:532–541
- Hackenberg J, Spiecker H, Calders K, Disney M, Raunonen P (2015) SimpleTree—An efficient open source tool to build tree models from TLS Clouds. *Forests* 6:4245–4294
- Herwitz SR (1985) Interception storage capacities of tropical rainforest canopy trees. *J Hydrol* 77:237–252
- Holder CD, Gibbes C (2017) Influence of leaf and canopy characteristics on rainfall interception and urban hydrology. *Hydrol Sci J* 62:182–190
- Holwerda F, Bruijnzeel LA, Scatena FN, Vugts HF, Meesters AGCA (2012) Wet canopy evaporation from a Puerto Rican lower montane forest: the importance of realistically estimated aerodynamic conductance. *J Hydrol* 414–415:1–15
- Kimbauer MC, Baetz BW, Kenny WA (2013) Estimating the stormwater attenuation benefits derived from planting four monoculture species of deciduous trees on vacant and underutilized urban land parcels. *Urban For Urban Green* 12:401–407
- Linoss AC, Siegert CM (2016) A comparison of five forest interception models using global sensitivity and uncertainty analysis. *J Hydrol* 538:109–116
- Livesley SJ, Baudinette B, Glover D (2014) Rainfall interception and stem flow by eucalypt street trees—the impacts of canopy density and bark type. *Urban For Urban Green* 13:192–197
- Levia DF, Herwitz SR (2005) Interspecific variation of bark water storage capacity of three deciduous tree species in relation to stemflow yield and solute flux to forest soils. *Catena* 64:117–137
- Levia DF, Keim RF, Carlyle-Moses DE, Frost EE (2011) Throughfall and stemflow in wooded ecosystems. Chapter 21 In: *Forest hydrology and biogeochemistry*. Ecological studies series 216. Springer, Heidelberg, pp 425–443
- McPherson GE, van Doorn N, de Goede J (2016) Structure, function and value of street trees in California, USA. *Urban For Urban Green* 17:104–115
- Miralles DG, Gash JHC, Holmes TRH, de Jeu RAM, Dolman AJ (2010) Global canopy interception from satellite observations. *J Geophys Res-Atmos* 115:D16122
- Monteith JL, Unsworth MH (2008) *Principles of environmental physics*. Academic Press, London
- Oliver HR (1971) Wind profiles in and above a forest canopy. *Q J R Meteorol Soc* 97:548–553
- Pereira FL, Gash JHC, David JS, Valente F (2009) Evaporation of intercepted rainfall from isolated evergreen oak trees: Do crowns behave as wet bulbs? *Agr For Meteorol* 149:667–679
- Pereira FL, Valente F, David JS, Jackson N, Minunno F, Gash JHC (2016) Rainfall interception modelling: Is the wet bulb approach adequate to estimate mean evaporation rate from wet/saturated canopies in all forest types? *J Hydrol* 534:606–615
- Raunonen P, Kaasalainen M, Åkerblom M, Kaasalainen S, Kaartinen H, Vastaranta M, Holopainen M, Disney M, Lewis P (2013) Fast automatic precision tree models from terrestrial laser scanner data. *Remote Sens* 5:491–520
- Rutter AJ, Morton AJ (1977) A predictive model of rainfall interception in forests. III. Sensitivity of the model to stand parameters and meteorological variables. *J Appl Ecol* 14:567–588
- Sadeghi SMM, Attarod P, Van Stan JT, Pypker TG (2016) The importance of considering rainfall partitioning in afforestation initiatives in semiarid climates: a comparison of common planted tree species in Tehran. *Iran Sci Total Environ* 568:845–855
- Smolander H, Stenberg P (1996) Response of LAI-2000 estimates to changes in plant surface area index in a Scots pine stand. *Tree Physiol* 16:345–349

- Stull R (2011) Wet-bulb temperature from relative humidity and air temperature. *J Appl Meteorol Climatol* 50:2267–2269
- Sypka P, Starzak R (2013) Simplified, empirical model of wind speed profile under canopy of Istebna spruce stand in mountain valley. *Agric For Meteorol* 171–172:220–233
- University of Georgia Weather Network (2016). <http://weather.uga.edu/>. Accessed 8 Aug 2016
- Valente F, David JS, Gash JHC (1997) Modelling interception loss for two sparse eucalypt and pine forests in central Portugal using reformulated Rutter and Gash analytical models. *J Hydrol* 190:141–162
- van der Ent RJ, Wang-Erlandsson L, Keys PW, Savenije HHG (2014) Contrasting roles of interception and transpiration in the hydrological cycle—Part 2: moisture recycling. *Earth Syst Dyn* 5:471–489
- van Dijk AIJM, Bruijnzeel LA (2001) Modelling rainfall interception by vegetation of variable density using an adapted analytical model. Part 1. Model description. *J Hydrol* 247:230–238
- van Dijk AIJM, Gash JHC, van Gorsel W, Blanken PD, Cescatti A, Emmel C, Gielen B, Harman LN, Kiely G, Merbold L, Montagnani L, Moors E, Sttornola M, Varlagin A, Williams CA, Wohlfahrt G (2015) Rainfall interception and the coupled surface water and energy balance. *Agric For Meteorol* 214–215:402–415
- Van Stan JT, Van Stan JH, Levia DF (2014) Meteorological influences on stemflow generation across diameter size classes of two morphologically distinct deciduous species. *Int J Biometeorol* 58:2059–2069
- Van Stan JT, Levia DF, Jenkins RB (2015) Forest canopy interception loss across temporal scales: implications for urban greening initiatives. *Prof Geogra* 67:41–51
- Van Stan JT, Lewis ES, Hildebrandt A, Rebmann C, Friesen J (2016) Impact of interacting bark structure and rainfall conditions on stemflow variability in a temperate beech-oak forest, Central Germany. *Hydrol Sci J* 61:2071–2083
- Wang J, Endreny TA, Nowak DJ (2008) Mechanistic simulation of tree effects in an urban water balance model. *J Am Water Resour Assoc* 44:75–85
- Wang-Erlandsson L, van der Ent RJ, Gordon LJ, Savenije HHG (2014) Contrasting roles of interception and transpiration in the hydrological cycle—part 1: temporal characteristics over land. *Earth Syst Dyn* 5:441–469
- Xiao Q, McPherson EG, Ustin SL, Grismer ME, Simpson JR (2000) Winter rainfall interception by two mature open-grown trees in Davis, California. *Hydrol Process* 14:763–784
- Xu X, Yi C, Kutter E (2015) Stably stratified canopy flow in complex terrain. *Atmos Chem Phys* 15:7457–7470

Reproduced with permission of copyright owner.
Further reproduction prohibited without permission.